J. Biochem. **144,** 399–408 (2008)
doi:10.1093/jb/mvn082

Gene Expression Profiling of Human Mesenchymal Stem Cells for Identification of Novel Markers in Early- and Late-Stage Cell Culture

Shihori Tanabe*, Yoji Sato, Takayoshi Suzuki, Kazuhiro Suzuki, Taku Nagao and Teruhide Yamaguchi#

Division of Cellular and Gene Therapy Products, National Institute of Health Sciences, Tokyo 158-8501, Japan

Received January 9, 2008; accepted June 5, 2008; published online June 11, 2008

Human mesenchymal stem cells (hMSCs) are multipotent cells that differentiate into several cell types, and are expected to be a useful tool for cellular therapy. Although the hMSCs differentiate into osteogenic cells during early to middle stages, this differentiation capacity decreases during the late stages of cell culture. To test a hypothesis that there are biomarkers indicating the differentiation potential of hMSCs, we performed microarray analyses and profiled the gene expression in six batches of hMSCs (passages 4–28). At least four genes [necdin homolog (mouse) (*NDN*), EPH receptor A5 (*EPHA5*), nephroblastoma overexpressed gene (*NOV*) and runt-related transcription factor 2 (*RUNX2*)] were identified correlating with the passage numbers in all six batches. The results showed that the osteogenic differentiation capacity of hMSCs is down-regulated in the late stages of cell culture. It seemed that adipogenic differentiation capacity was also down-regulated in late stage of the culture. The cells in late stage are oligopotent and the genes identified in this study have the potential to act as quality-control markers of the osteogenic differentiation capacity of hMSCs.

Key words: cellular therapy, culture stage marker, differentiation, gene expression, stem cell.

Abbreviations: EPHA5, EPH receptor A5; hMSCs, human mesenchymal stem cells; NDN, necdin homolog (mouse); NOV, nephroblastoma overexpressed gene; PBS, phosphate buffered saline; RUNX2, runt-related transcription factor 2.

INTRODUCTION

'Cellular therapy' is a new concept in treating diseases with cells that have regeneration potential. Currently, it is at the clinical research stage; however, the use of cellular therapeutics in regular clinical settings will be implemented in near future. Cellular therapeutics involves the use of cells derived from human tissue, either cultured and/or modified, in regenerating and repairing damaged tissues and consequently improving the functions in the human body. Hence, tissue or embryonic stem cells that have the potential to differentiate into a variety of cell types are one of the prime candidate cells for cellular therapeutics. It is difficult to overview the entire discipline of cellular therapeutics since the cells themselves represent 'life'.

Stem cells, one of the candidates for cellular therapeutics, produce daughter cells identical to themselves that differentiate into other types of cells (*1*). The fate of the stem cells is determined by cellular signaling, although the underlying mechanism is still unknown. It is therefore important to investigate the gene expression patterns that influence the cellular signaling pathways and identify the representative biomarkers that can act as indicators of the differentiation potential of the stem cells. Recently, it has been reported that human somatic cells can be induced to pluripotent stem cells (*2*).

There have been several reports suggesting that cellular therapeutics is a promising treatment for several diseases. C-kit-expressing cells obtained from the bone marrow have been used in cardiac tissue repair in mice experiments (*3*). Previous studies have reported the use of autologous bone marrow cells transplantation for the post-infarction recovery of cardiac function (*4–9*). Cytotoxic T cells have also been used for cellular therapy to protect from infectious diseases in an immunodeficient condition following hematopoietic stem cell transplantation (*10*). Mesenchymal stem cells (MSCs) are also used for therapy expecting immunosuppressive effects (*11, 12*). Previous studies on MSCs also indicate that these cells possess the ability for chondrogenic (*13*), osteogenic (*14, 15*) and adipogenic differentiation, and possibly other differentiating capabilities (*16*). In a clinical setting, it is difficult to assess the overall profile of each batch of the cells. We hypothesized the existence of quality-control markers for the differentiation potential of human mesenchymal stem cells (hMSCs) and used gene expression profiling to identify these markers.

*To whom correspondence should be addressed. Tel: +81-3-3700-1141, Fax: +81-3-3700-9217, E-mail: stanabe@nihs.go.jp
#Present address: Division of Biological Chemistry and Biologicals, National Institute of Health Sciences

EXPERIMENTAL PROCEDURES

Cell Culture—The hMSCs derived from bone marrow [Lonza (Cambrex), Walkersville, Maryland, USA] were cultured in mesenchymal stem cell growth medium (MSCGM) [Lonza (Cambrex) #PT-3001; mesenchymal stem cell basal medium supplemented with mesenchymal cell growth supplement, L-glutamine and penicillin/streptomycin] at 37°C in CO_2 (5%) incubator. Cells were passaged according to the manufacturer's protocol with slight modification using trypsin–EDTA solution [Lonza (Cambrex) #CC-3232]. Lot numbers of the hMSC batches were as follows: #4F1127, #4F0312, #5F0138, #4F1560, #4F0591 and #4F0760. Informed consent was obtained in Poietics human mesenchymal stem cell systems [Lonza (Cambrex)]. All differentiation procedures were performed according to Lonza (Cambrex) protocol with slight modification.

Osteogenic Differentiation—The hMSCs were plated onto 12-well plates and 24 h later, the medium was changed to MSCGM (as control) or osteogenic induction medium (OIM) [Lonza (Cambrex) #PT-3002; differentiation basal medium containing dexamethasone, ascorbate, mesenchymal cell growth supplement, L-glutamine, penicillin/streptomycin and β-glycerophosphate]. Medium was changed every 3–4 days and cells were differentiated for 21 days.

Calcium Deposition Assay—Calcium deposition was measured using the Stanbio Total Calcium Liquicolor® kit (Stanbio Laboratory, Boerne, Texas, USA; #0150-250) according to the manufacturer's protocol (Cambrex, Stanbio Laboratory). Briefly, the cells cultured on 12-well plates for 22 days (osteogenic-induced for 21 days) were rinsed with phosphate buffered saline (PBS) without calcium and magnesium [Lonza (Cambrex) #17-516Q] and harvested in 0.5 N HCl (600 µl). Calcium was extracted from the cells by shaking the tubes for approximately 20 h at 4°C. Lysates were centrifuged at 500*g* for 2 min at 4°C and 20 µl of the supernatant was used for the assay. Absorption at 560 nm was measured to detect the Ca-ortho-cresolphthalein complexone (OCPC) complex using an EnVision 2103 multilabel reader (PerkinElmer, Waltham, Massachusetts, USA). Calcium deposition was adjusted with the total protein concentration of the samples. Cells harvested in 0.5 N HCl were centrifuged at 15,000 rpm for 10 min at 4°C. The pellet was washed once with PBS without calcium and magnesium, and resuspended in 100 µl of 0.1 N NaOH/0.1% SDS. After overnight incubation at 37°C, the lysate was centrifuged at 15,000 rpm for 10 min at room temperature, and the supernatant was quantitated using the DC protein assay (Bio-Rad Laboratories, Hercules, California, USA) according to the manufacturer's protocol. Absorbance at 620 nm was measured using the EnVision 2103 multilabel reader (PerkinElmer). The standard curve was obtained using bovine serum albumin.

Adipogenic Differentiation—The cells were plated onto a 24 well-plate at 2.1 x $10^4/cm^2$, and cultured in MSCGM for 5–6 days. After cells reach confluence, medium was changed to MSCGM (as control) or adipogenic induction medium (AIM) [Lonza (Cambrex) #PT-3004; induction basal medium supplemented with recombinant human insulin, L-glutamine, mesenchymal stem cell growth supplement, penicillin/streptomycin, dexamethasone, indomethacin and IBMX (3-Isobutyl-1-methylxanthine)]. Medium was changed after 3 days into adipogenic maintenance medium (maintenance basal medium supplemented with recombinant human insulin, L-glutamine, penicillin/streptomycin and mesenchymal stem cell growth supplement). After three complete cycles of induction/maintenance, the cells were cultured for 7 more days in adipogenic maintenance medium, replacing the medium every 2–3 days.

Oil Red O staining—The cells were rinsed with 500 µl of PBS and fixed with 10% neutral buffered formalin (500 µl). After washing with sterile water, the cells were washed with 60% 2-propanol (500 µl) for 2–5 min and stained with Oil Red O (500 µl) for 5 min. The cells were rinsed with tap water and stained with Harris' haematoxylin (500 µl) for 1 min and rinsed with the water. Lipid vesicles were observed with microscope Biozero BZ-8000 (KEYENCE, Osaka, Japan).

Chondrogenic Differentiation—The cells (3×10^5) were washed with incomplete chondrogenic induction medium [Lonza (Cambrex) #PT-3003; chondrogenic basal medium containing dexamethasone, ascorbate, ITS (insulin-transferrin-sodium selenite) + supplement, sodium pyruvate, proline, penicillin/streptomycin, L-glutamine] and were resuspended in 0.5 ml of complete chondrogenic induction medium (CCIM; incomplete condrogenic induction medium supplemented with 10 ng/ml of TGF-β3) or MSCGM (as control) and cultured in 15 ml polypropylene culture tubes. The medium was replaced every 3–4 days and the cells were cultured for 24 days.

Safranin-O Stains for in vitro Chondrogenesis—The chondrogenic pellets were fixed in 10% neutral buffered formalin and paraffin embedded. The paraffin sections were stained with Weigert's iron hematoxylin (Wako 298-21741), 0.02% fast green FCF (MP biomedicals 195178) and 0.1% Safranin-O (Sigma HT 90432), followed by observation with microscope Biozero BZ-8000 (KEYENCE).

Total RNA Purification—The hMSCs were cultured on a 10 cm dish, lysed in 600 µl of Buffer RLT (RNeasy® Lysis Buffer) with β-mercaptoethanol and homogenized using a QIA shredder (QIAGEN, Düsseldorf, Germany). Total RNA was purified using RNeasy® mini spin columns according to manufacturer's protocol (QIAGEN). Total RNA was eluted with RNase-free water.

Microarray Analysis—Total RNA (100 ng or 1 µg) was reverse transcribed and amplified using a GeneChip® kit (Affymetrix, Santa Clara, California, USA) and the biotinylated cRNA was hybridized onto the GeneChip® Human Genome U133 Plus 2.0 Array (54,613 probe sets). The data was analysed using GeneChip Operating System software (versions 1.2–1.4), followed by statistical analysis. The data was also analysed using GeneSpring™ (version 7.3) (Agilent, Santa Clara, California, USA). The data discussed in this publication have been deposited in NCBI's Gene Expression Omnibus (GEO; http://www.ncbi.nlm.nih.gov/geo/) (*17*, *18*). They are accessible through GEO Series accession number GSE7637 for the data from 4F1560, and GSE7888 for the data obtained from all six batches. The statistical method for microarray data analysis has been also discussed elsewhere (*19*).

Cluster Analysis—The microarray data of 169 probe sets obtained from six batches of hMSCs was subject to cluster analysis using the Gene Expression Statistical System (NCSS, Kaysville, Utah; Dr Jerry L. Hintze). Fold change of signal intensity to the average signal intensity of early stage was analysed and a double dendrogram was plotted on a log 2 scale.

Gene Ontology Analysis—Gene ontology analysis was conducted using Ingenuity Pathway Analysis (IPA) (Ingenuity® Systems, Redwood City, California, USA), NetAffyx (Affymetrix) and GOTM (Gene Ontology Tree Machine, Vanderbilt University, Nashville, Tennessee, USA) analyses. Probe sets with signal intensity values associated with the passage numbers were subject to analyses. The functional analysis identified the biological function and/or diseases that were most significant to the data set. Genes from the data set that were associated with biological functions and/or diseases in the Ingenuity Pathways Knowledge Base (IPKB) were considered for further analysis.

cDNA Synthesis and Real-time PCR Using Taqman Low-density Array—RT–PCR (reverse transcriptase–PCR) analysis was performed to assess the mRNA levels in six batches of hMSCs using TaqMan® low-density array (TLDA) (Format 48) (Applied Biosystems, Foster City, California, USA). The data was normalized using *GAPDH* (glyceraldehyde-3-phosphate dehydrogenase). Forty-six genes including *GAPDH* as endogenous control are listed in Supplementary Table 1. cDNA was synthesized using a High-capacity cDNA synthesis kit (Applied Biosystems) and Multiscribe reverse transcriptase. cDNA synthesized from 100 ng of total RNA was used for the analysis (2 ng of total RNA per well). Real-time PCR was analysed using 7900 HT real-time PCR system (Applied Biosystems). The conditions for the PCR reaction were as follows: 50°C (2 min) and 94.5°C (10 min), and 40 cycles at 97°C (30 sec) and 59.7°C (1 min). Relative quantification values were calculated by the comparative Ct method using SDS 2.2.2 software (Applied Biosystems).

Pathway Network Analysis—Data were analysed using the IPA (Ingenuity® Systems, www.ingenuity.com). A data set containing gene identifiers and corresponding expression values was uploaded into the application. Each gene identifier was mapped to its corresponding gene object in the IPKB. A fold-change cutoff of 3 for both up- and down-regulation and a p-value cutoff of 0.05 were set to identify the genes to be analysed. These genes, called focus molecules, were overlaid onto a global molecular network developed from information in the IPKB. Networks of these focus molecules were then algorithmically generated based on their connectivity. The functional analysis of a network identified the biological functions and/or diseases that were most significant to the genes in the network. The genes in the networks associated with biological functions and/or diseases in the IPKB were considered for the analysis. Genes and gene products are represented as nodes, and the biological relationship between two nodes is represented as an edge (line). All edges are supported by at least one reference from the literature, textbook or canonical information stored in the IPKB. Human, mouse and rat orthologs of a gene are stored as separate objects in the IPKB, but are represented as a single node in the network. The node colour indicates the degree of up- (red) or down- (green) regulation. Nodes are displayed using various shapes that represent the functional class of the gene product.

Statistical Analyses—Non-parametric analysis was used for microarray data analyses. The Spearman correlation coefficient and two-tailed p-values were calculated. $P<0.001$ or $P<0.05$ were considered to be significant. RT–PCR data was analysed with non-parametric analysis. The Spearman correlation coefficient and two-tailed p-values were calculated. To compare the specific passage number and stage, Student's t test was performed. Two-way ANOVA followed by Bonferroni post-test was performed for osteogenesis data. GraphPad Prism® 4 and Microsoft® Office Excel were used for statistical analysis and drawing graphs.

RESULTS

Microarray Analysis of hMSCs—To identify the quality-control markers in different stage of the culture, we performed DNA microarray analyses. Non-parametric analysis and a ratio (max/min of signal intensity) cutoff of 3.071,524 ($1.05^{(28-5)}$; 5% change in each passage from 5th to 28th) showed that the expression level of 341 probe sets out of a total of 54,613 probe sets had a significant association with passage numbers (hMSC lot #4F1560, passage numbers 5, 7, 9, 13, 21 and 28).

Gene ontology analyses showed that the mapped genes corresponded to the probe sets belonging to various categories of molecular and cellular functions such as cell-to-cell signaling and interaction, cellular movement, cell death, cellular assembly, cellular organization and cell cycle, and physiological system development, and biological functions such as hematological system development and function, immune and lymphatic system development and function, tissue development, immune response and embryonic development. The top five disease categories that the genes mapped to, as identified using the IPA software, included cardiovascular, hematological, musculoskeletal, oncogenic and reproductive disorders.

Figure 1 shows the results of cluster analysis obtained from microarray data of six batches of hMSCs in early (passage #4–5), middle (#7–9) and late stages (#22–28). Seventy-nine genes out of the 169 probe sets were categorized by function and disease as per IPA analysis. Networks were analysed for each of the six batches and a representative network is shown in the Supplementary Fig. 1. A list of all top networks in each analysis is shown in Table 1. Many network categories with the top score in each analysis were involved in cancer or regulation of cell cycle. Additionally, specific networks for each sample were generated when the batches were individually analysed.

Calcium Deposition of Osteogenic-induced Cells—In Fig. 2, calcium deposition in hMSC cultures (4F0312, 5F0138, 4F1560, 4F0591, 4F0760) were measured during passages 7, 9, 10 and 19. The results showed that the osteogenic differentiation occurred in early to middle stages and was dramatically suppressed during the late

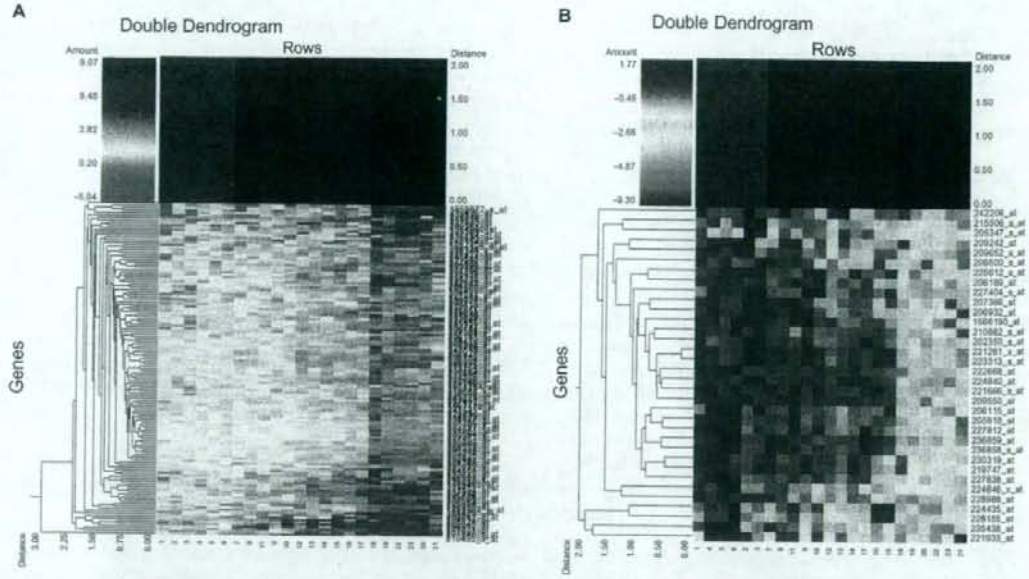

Fig. 1. **Microarray analysis of hMSCs.** One hundred and sixty-nine probe sets extracted from microarray data of six batches of hMSCs. [$n=6$ in early stage (#4 or 5), passage #9, late stage (#22, 24 or 28), $n=5$ in passage #7]. Cut off value of signal intensity ratio (max/min of average in each stage) is 2.949145023 [5% change in each passage number from early to late stage; 1.05 (passage number range of average in early and late stage)]. Double dendrograms of up-regulated 135 probe sets (A) and down-regulated 34 probe sets (B) are shown.

stages of cell culture. These findings suggest that the expression levels of genes associated with osteogenesis are different at the late stages compared with those at earlier stages of cell culture.

Statistical analysis of microarray and calcium deposition data from three batches (5F0138, 4F1560, 4F0591) of hMSCs in middle (#7–10) and late (#19–28) stages showed that the expression of *NDN* [necdin homolog (mouse)] has a positive correlation with calcium deposition ($P<0.05$).

Adipogenic Differentiation of hMSCs—Figure 3A shows the results of Oil Red O staining of adipogenic-induced cells. The cells were adipogenic induced for 21 days and lipid was stained with Oil Red O. Adipogenesis of hMSCs seemed to be down-regulated in late culture stage of 5F0138, 4F0591 and 4F0760, while the adipogenic-differentiation capacity seemed to be retained in passage #20 of 4F1560.

Chondrogenic Differentiaion of hMSCs—Figure 3B shows the Safranin-O staining of chondrogeninc-differentiated hMSCs. The cells were differentiated in CCIM for 24 days and stained with Safranin-O. The culture in passages 7, 17 and 22 of 4F0591 showed chondrogenic-differentiated morphology (a, b, c, respectively). The culture in late stage seemed to be chondrogenic differentiated as shown (c). The cells cultured in MSCGM as control did not show any chondrogenic-differentiated morphology (d).

RT-PCR Analysis of hMSCs—The quantitative RT–PCR data showed that some genes had similar expression profiles in all the six batches examined. Up-regulated genes, which were identified as candidates for the stage-specific markers included *EPHA5* (EPH receptor A5), *NOV* (nephroblastoma overexpressed gene), *SERPINE1* [serpin peptidase inhibitor clade E (nexin, plasminogen activator inhibitor type 1), member 1], *ITGA4* [integrin, alpha 4 (antigen CD49D, alpha 4 subunit of VLA-4 receptor)], and down-regulated genes, which are also candidates for the stage-specific markers included *NDN*, *RUNX2* (runt-related transcription factor 2) and *RUNX3* (runt-related transcription factor 3). *NOV* is a growth factor and is involved in the proliferation of bone cancer cell lines (*20*). It is notable that the expression of *NOV* in lot #4F1127 was relatively stable. *SERPINE1* is involved in the protein-binding function and diseases such as heart failure (*21*). *RUNX2* is a member of the runt domain-containing family of transcription factors and suggested to regulate osteogenic differentiation (*22*). *RUNX3* is also a member of the runt domain-containing family of transcription factors and a candidate tumor suppressor (*23*). *EPHA5*, *NOV*, *NDN* and *RUNX2* showed altered expression correlating with passage numbers ($P<0.01$) (Fig. 4). The results of RT–PCR analysis of 45 genes examined are shown in Supplementary Fig. 2.

DISCUSSION

hMSCs will be used for cellular therapeutics in clinical settings in the near future. The importance of quality control of the cells will be significant as the use of cellular therapeutics becomes more common. In this report, we report on profiling the gene expression of

Table 1. **List of the networks in hMSCs.**

Analysis	Molecules in network	Score	Focus molecules	Top functions
4F0591-#9	BUB1B, CCNB1, CDC2, CDKN3, CENPF, CGREF1, Cyclin E, DLG7, E2f, ERCC6L, FOXM1, KRT8, LRP1, MAD2L1, MEOX2, NDC80, NFkB, NUF2, NUSAP1, OLR1, PBK, PCSK1, PLK1, PTTG1, RAD51AP1, Rb, RNA polymerase II, RRM2, SERPINB2, SPC25, TFPI2, TNFSF9, TRADD, TYMS, UBE2C	65	30	Cell Cycle, Cancer, Reproductive System Disease
4F1560-#28	ADH1B, ALDH1A3, BEX1 (includes EG:55859), BMP15, CD80, CHI3L1, DBP, DLX1, ENPP1, FGF5, GBP2, IGF2, Igfbp, IGFBP5, KRT19, LBP, MEOX2, Mmp, NFkB, NOV, PCSK1, PCSK5, PEG10, PYCARD, RAGE, SEPP1, SERPINB2, SERPING1, ST8SIA1, Tgf beta, TLR1, TNFAIP6, TNFSF15, TRAF4, TSLP	57	31	Cancer, Cellular Growth and Proliferation, Neurological Disease
4F0760-#9	ANKRD1, Ap1, BIRC3, CCNB1, CCR2, CDC2, CENPE, COL15A1, FBLN5, Jnk, LATS1, Mmp, MSR1, NDC80, NFkB, NRL, NUF2, OMD, PBK, Pdgf, PDGF BB, PDGFD, PRDM1, S100A4, SERPINB2, SLC37A4, SORBS3, SPC24, SPC25, TFPI2, THBD, TNFRSF8, VANGL2, VAV3, VSNL1	56	29	Cancer, Cell Cycle, Reproductive System Disease
5F0138-#24	ARL4C, BUB1 (includes EG:699), BUB1B, CCNB1, CCNB2, CCNF, CDC2, CDC7, CDC20, CDC25C, CDKN3, CENPE, CENPH, Cyclin B, Cyclin E, FBXO5, FOXM1, GINS1, GPNMB, IL6, KIAA0101, KIF11, KIF22, KIF2C, MRVI1, NDC80, NUF2, PBK, PLK4, PTTG1, SLC7A7, SPC25, UBE2C, VTCN1, ZWINT (includes EG:11130)	52	33	Cell Cycle, Cancer, DNA Replication, Recombination, and Repair
4F1560-#9	14-3-3, AURKA, BIRC5, CCNB1, CDC20, CDC25C, CDCA8, Cyclin B, Cyclin E, E2f, IGF2, MAD2L1, NDC80, NFkB, NUF2, OLR1, PBK, PRR11, RAD51AP1, Rb, RGS7, RNA polymerase II, RRM2, Scf, SERPINB2, SFN, SFRP4, SPC24, SPC25, TNFRSF8, TOP2A, TYMS, UBE2C, UHRF1, ZNF74	52	27	Cancer, Cell Cycle, Reproductive System Disease
4F0591-#28	AEBP1, ALDH1A3, ANGPT1, ANKRD1, BEX1 (includes EG:55859), C1R, CGREF1, CXCL16, DIRAS3, GAD1, HDAC9, ID4, IL1, IL1R1, KRT18, KRT19, MEOX2, Mmp, MYBL1, MYPN, NFkB, OLR1, PAK1IP1, Pdgf Ab, PLAT, PYCARD, RIPK4, SERPINB2, SERPINF1, SERPING1, TFPI2, Tgf beta, TNFRSF19, TNFRSF11B, TSLP	51	30	Cancer, Cardiovascular Disease, Cell Death
4F0312-#7	A2M, ACAN, ASPN, BRCA1, C1R, C1S, CEBPD, CYP27A1, DDIT3, DDIT4, ESR1, FGF7, GDF15, IL1, Jnk, KSR2, MAD2L1, Mek, Mek1/2, Mmp, NFkB, NOTCH3, NOX4, NR4A1, OSMR, P38 MAPK, PCK2, Pdgf, PDGF BB, SERPINB2, STAT, TNFAIP6, TNFSF9, TNFSF15, TRIB3	50	25	Cell Cycle, Inflammatory Disease, Cellular Development
4F0312-#28	ANKRD1, BEX1 (includes EG:55859), BLK, CD36, CDKN2B, CTSL2, ENPP1, F2RL1, FABP5, FKBP5, FUS, G0S2, GAD1, GDF15, IGFBP5, IGHG1, IL1, N-cor, NFkB, OLR1, PAPPA2, PLAT, PNRC1, Rxr, RXRA, SERPINB2, STMN2, Tgf beta, THRB, Thyroid hormone receptor, TNFRSF19, TNFRSF11B, TNFSF13B, TRIP13, VSNL1	50	29	Cancer, Cellular Growth and Proliferation, Immunological Disease
4F1560-#7	14-3-3, AURKA, BIRC5, CCNE2 (includes EG:9134), CDC25A, CDCA8, CEBPA, CENPF, CSPG4, Cyclin A, Cyclin E, E2f, ESPL1, FEN1, FMOD, Histone h3, Mapk, MCM8, MCM10, MDM4, NUSAP1, OIP5, PP2A, PRR11, PTTG1, Rb, RGS7, RRM2, SFRP4, SMPDL3A, SOS2, TOP2A, TTK, TYMS, UBE2C	50	27	Cell Cycle, Cancer, Reproductive System Disease
4F0312-#9	ABCA1, ACAN, AEBP1, Akt, ANXA11, ASPN, C1R, C1S, CD36, DKK, F2RL1, FBLN1, FGF7, FOXE1, GDA, GDF15, HSD11B1, IGF2, IGFBP2, Insulin, LDL, LEPR, Mapk, NFkB, NTF3, P38 MAPK, PDGF BB, PTX3, SLC7A7, THBS2, TNFAIP6, TNFSF9, Wnt, WNT2, WNT16	49	23	Lipid Metabolism, Molecular Transport, Small Molecule Biochemistry

(continued)

Table 1. **Continued.**

Analysis	Molecules in network	Score	Focus molecules	Top functions
5F0138-#9	ABCA1, AEBP1, ARG2, BGN, C1q, C1R, C1S, CYP2B6 (includes EG:1555), DDIT4, ENPP1, FABP5, FADS1, GDF15, HABP2, N-cor, NCOR-LXR-Oxysterol-RXR-9 cis RA, NFkB, Nr1h, OLR1, PCK2, PDGF BB, PTGDR, Rxr, SCD, SERPING1, SFTPD, SORBS3, SREBF1, SYNE1, THBS2, Thyroid hormone receptor, TNFAIP6, TNFSF9, TRIB3, VDR	46	27	Respiratory Disease, Inflammatory Disease, Lipid Metabolism
4F1127-#9	ACAN, Alkaline Phosphatase, Ap1, ASPN, C3, CCL2, CCNO, COL13A1, CP, FABP5, GEM, HMOX1, HOMER2, IGFBP5, IL1, JAG1, LDB3, LDL, Mmp, MMP28, NFkB, P38 MAPK, Pdgf, PDGF BB, RGS4, SERPINB2, SPINT2, SPP1, TAC1, Tgf beta, TNFAIP6, TNFRSF11B, TXNIP, VitaminD3-VDR-RXR, ZNF335	45	24	Cellular Development, Cellular Growth and Proliferation, Skeletal and Muscular System Development and Function
4F1127-#22	AEBP1, ANKRD1, C1q, C1R, CBR3, CD36, CFH, ENPP1, FLNC, FOXF1, G0S2, HAMP, HDL, HIST2H2AA3, HIST2H2BE, HIVEP1, IGKC, KCNAB1, KCND2, KRT17, LDB3, LY6E (includes EG:4061), MYOZ1, NFkB, OLR1, PLK3, POU2F2, REG3A, RIPK4, SLC40A1, TNFRSF19, TNFRSF10D, TNFSF9, TSLP, VSNL1	44	32	Genetic Disorder, Metabolic Disease, Molecular Transport
4F0760-#28	Alpha Actinin, CDH1, CTSH, Cyclin A, Cyclin E, E2f, EDN1, GAST, ICAM2, Integrin, ITGA2, ITGA6, KRT7, KRT18, LAMC2, MARCKSL1, Mek1/2, Mmp, MYOZ2, OCLN, PCOLCE, PCOLCE2, Plc beta, PLCB4, PRPS1, Rb, S100A4, SCG5, SDPR, SERPINB2, SMURF2, TFPI2, TGFB1, TNFRSF11B, TSPAN8	44	26	Cardiovascular System Development and Function, Cell Morphology, Skeletal and Muscular System Development and Function
4F0591-#7	AMELX, AQP4, ARNT2, BAT3, beta-estradiol, BIRC5, CATSPERB, CDCA8, CEBPA, CGREF1, DLGAP1, GLIPR1, GPR37, GRIN1, GTSE1, HSPA2, HSPA5, INS1, LITAF, NCAPG (includes EG:64151), NFkB, NPAS1, PLGLB2, RAB31, RAGE, retinoic acid, RPS14, RPS4X, RRM2, SCG2, STXBP4, TF, TGFBI, TP53, TRHDE	38	16	Cell Death, Cancer, Respiratory Disease
4F1127-#7	Actin, ADIPOQ, Akt, Ap1, BCL9, BIRC5, CCL2, CPE, EGR2, ERCC6L, HIST1H4C, Histone h3, HOMER2, IL1, IL8, Jnk, KRT18, LDL, NFkB, OSBP, P38 MAPK, PBK, PDGF BB, PDGFC, PLK1, POSTN, PRDX4, SERPINA3, SFRP4, SLC2A3, Tgf beta, TIFA, TNFRSF11B, TNFRSF1B, TPT1	35	17	Cellular Growth and Proliferation, Cellular Development, Hematological System Development and Function
5F0138-#7	Akt, Ap1, ASNS, CALM2, DAD1, DDIT4, FSTL1, G0S2, GARS, GDF15, HTRA1, JAK3, LDHA, LDL, LOX, MMP1 (includes EG:4312), NFkB, P38 MAPK, PCK2, PCOLCE, PDGF BB, PDGFC, PDPN, RND3, RPN2, SFRP1, SLC7A1, TCR, TGFB1, TIMP4, TNFRSF8, TNFSF9, TRIB3, UGDH, WNT2	30	15	Cancer, Cellular Movement, Cellular Development

The top networks in each analysis data analyzed by IPA are listed.

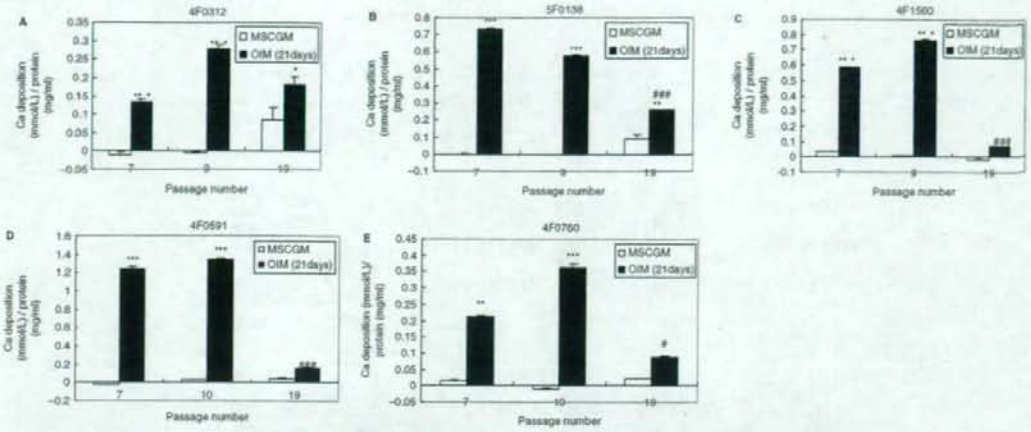

Fig. 2. **Calcium deposition of hMSCs.** The cells in each passage numbers indicated were plated on 12-well plates and cultured in MSCGM (control; clear column) or OIM (osteogenic differentiated; filled column) for 21 days. The amounts of calcium deposition in 4F0312, 5F0138, 4F1560, 4F0591 and 4F0760 are indicated in (A, B, C, D and E), respectively. Calcium deposition divided by protein concentration is showed as mean + SEM in triplicate. $^{***}P<0.001$, $^{**}P<0.01$, $^{*}P<0.05$ when osteogenesis in MSCGM was compared to that in OIM in each passage number. ### $P<0.001$, ## $P<0.01$, # $P<0.05$ when osteogenesis in passage #19 was compared to that in passage number 7 ($n=3$).

hMSCs through early and late stages of cell culture. Replication was performed by testing six different batches of cells. All six batches examined showed a marked decrease in culture growth rate with increasing passages.

The hMSC potential for osteogenic differentiation was down-regulated in all the batches of hMSCs examined during the late culture stage. The osteogenic differentiation was observed in all the batches of hMSCs examined for passages 7, 9 and 10. Also, every batch examined showed a down-regulation of the osteogeneic process during the 19th passage. As previously stated, four genes, *NDN*, *EPHA5*, *NOV* and *RUNX2* showed altered expression depending on the culture stage. *EPHA5* and *NOV* were up-regulated as the cells were further passaged, while *NDN* and *RUNX2* were down-regulated.

RT–PCR data indicated that the expression of *NDN* in all batches examined decreased during the late stages of culture. The expression of *NDN* in lot #4F1127, #4F0312 and #5F0138 was relatively stable until the 14th passage, which was then followed by a decrease in expression during the late stages. Microarray data also showed that the expression of *NDN* in passages 22–28 were decreased compared to that in passages 4–8. Furthermore, our results showed a positive correlation between the expression of *NDN* in hMSCs and the potential to differentiate into osteogenic cells as measured by the calcium deposition rates. Previous reports suggested that necdin, an *NDN* homolog, interacts with IL-1α precursor (*24*). The expression of *NDN* in hMSCs decreases with increasing passages. It is possible that *NDN* down-regulation is involved in activation of IL1-Myd88 pathway by dying cells (*25*).

Every batch showed a passage-dependent increase in the expression level of *EPHA5*. EPHA5 is transmembrane receptor protein tyrosine kinase, known as Ephrin A5 receptor, and belongs to the ephrin receptor subfamily. Recently, it has been shown that EPHA5 is involved in cellular growth and tumor malignancies (*26*, *27*). Also, it is known that the expression level of human *EPHA5* mRNA is high in primary human breast carcinoma cells (*28*).

NOV/CCN3 is a growth factor that plays several roles in cellular migration, growth, proliferation and chemotaxis. The previous finding that *NOV* inhibits the proliferation of a cancer cell line is consistent with the observation that *NOV* expression level is increased in the senescing phase, which coincides with the low proliferative stage of hMSCs. Furthermore, in primary skin fibroblasts, NOV/CCN3 protein increases the expression of human *SERPINE1* mRNA level (*29*). This is consistent with our observation that the expressions of *SERPINE1* as well as *NOV* are up-regulated during the late stages of cell culture. Mutant human SERPINE1 (T333R; A355R), which lacks the protease-inhibitory activity, decreases the quantity of rat laminin and inhibits matrix accumulation (*30*). On the other hand, previous finding indicated that the expression of mouse *Myod1* (myogenic differentiation 1) mRNA level and Myog (myogenin) protein decreased in C2/4 cells (subclone of C2C12 mesenchymal cells) stably expressing NOV, which suggests that NOV suppresses the myogenic differentiation of C2/4 cells (*31*).

The expression of *RUNX2* was also decreased in late stage of the culture. *RUNX2* is a member of the runt family of transcription factors and suggested to be involved in osteogenesis (*22*). It is possible that down-regulated osteogenic differentiation of hMSCs is caused by the decreased expression of *RUNX2*. Recent reports have shown that 3D cultures of human adipose tissue-derived endothelial and osteoblastic progenitors generate osteogenic–vasculogenic constructs (*32*). It might be

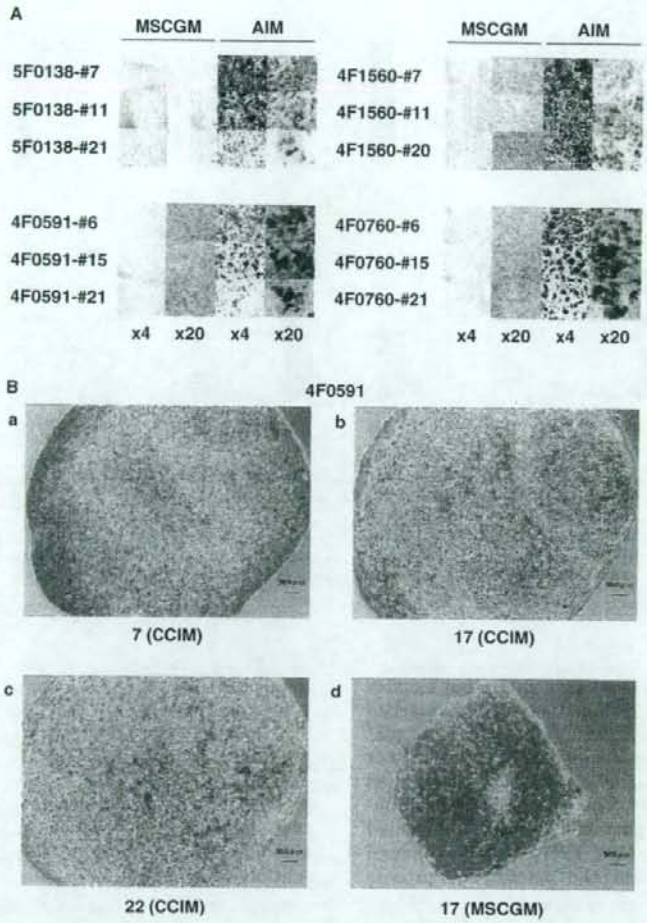

Fig. 3. **Adipogenic differentiation and chondrogenic differentiation of hMSCs.** (A) The cells in each passage numbers indicated were plated on 24-well plates and cultured in MSCGM (as control) or AIM (adipogenic differentiation medium) for 21 days. The cells were stained with Oil Red O. (B) The cells in passage. #7, #17 or #22 of 4F0591 were cultured in CCIM for 24 days and stained with Safranin O (a, b, c, respectively). Proteoglicans stained red. The cells in passage #17 were also cultured in MSCGM (as control) for 24 days (d).

interesting to investigate the gene expression profile of the 3D culture of hMSCs.

In conclusion, microarray and RT–PCR data of the six batches of hMSCs suggested that four genes, *EPHA5*, *NOV*, *NDN* and *RUNX2* have the potential to act as stage-specific markers during hMSC culture. These genes can be used as candidates for quality control markers of the culture status with regard to the differentiation potential for future clinical application of hMSCs for cellular therapeutics. We reported that the capacity of hMSCs for osteogenic differentiation was highly suppressed during the late culture stages. *NDN* or *RUNX2* may be a quality control marker of hMSC capacity for osteogenic differentiation. The observations of adipogenic differentiation of hMSCs suggested that each batch shows different transition in differentiation potential. It seemed that the capacity tends to be suppressed in late stage of the culture. The observations of chondrogenic differentiation suggested that the differentiation potential of hMSCs is retained in late stage of the culture. It seems that the cells in the late stage have limited differentiation potential (oligopotent). Furthermore, network analysis and gene expression analysis revealed that the expression profiles are distinct for each passage number. These findings imply the importance of quality control for safe application of hMSCs for cellular therapy and usefulness of expression analysis for finding marker genes. Phenotype profiling and profiling at the genome level, including chromosomal analysis, might need more research in the future. The profiling of the cells, in both differentiated and 3D states, will also need to be investigated for future clinical applications.

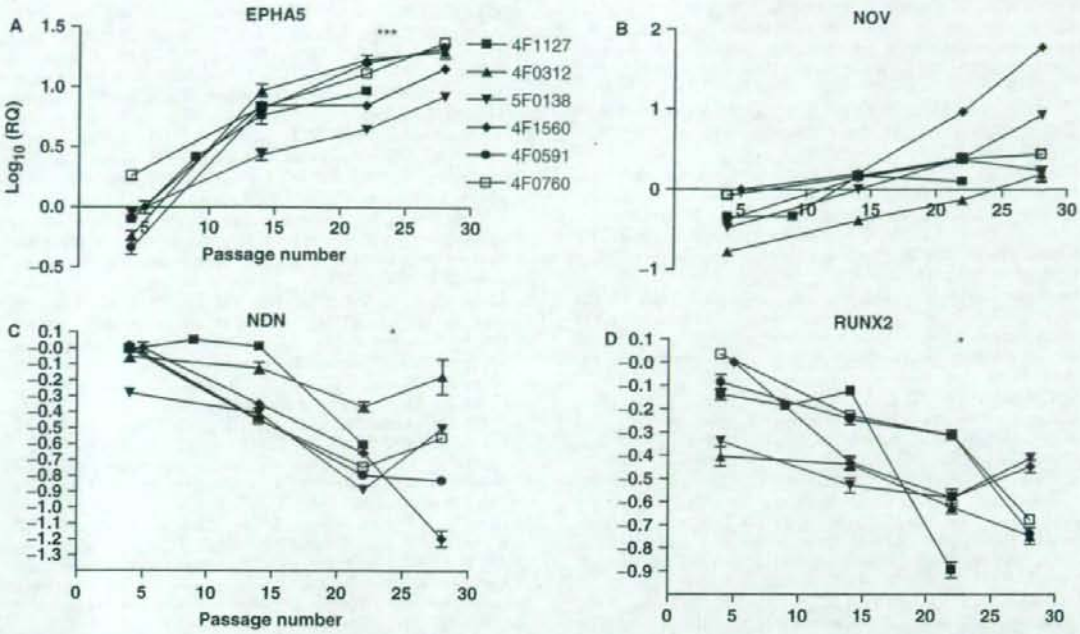

Fig. 4. **Gene expression profiles of culture stage markers suggested for hMSCs.** Individual plots for six batches of hMSCs obtained from RT–PCR data. The expression of *EPHA5* (A), and *NOV* (B) increased, while that of *NDN* (C) and *RUNX2* (D) decreased as the cells were further passaged in each batch. Relative quantity value was plotted on a log 10 scale. The expression of four genes (A–D) was correlated with passage numbers ($P < 0.01$). *** $P < 0.001$, * $P < 0.05$ when the expression in passage #14 was compared to that in late stage (passage #22 and #28) ($n = 6$ in passage #14, $n = 10$ in late stage).

Supplementary data are available at *JB* online.

We thank Dr Y. Hayashi for advice in microarray statistics analysis, and Dr Y. Shinozaki for assistance in microarray experiments. We are also thankful to Dr Y. Ohno and Dr E. Uchida for their support and valuable comments. We are most grateful to C. Aoyagi for her excellent skill in making paraffin sections. This work was supported in part by grants and the Grant-in-Aid for Cancer Research from the Ministry of Health, Labour and Welfare.

REFERENCES

1. Clevers, H. (2005) Stem cells, asymmetric division and cancer. *Nat. Genet.* **37**, 1027–1028
2. Takahashi, K., Tanabe, T., Ohnuki, M., Narita, M., Ichisaka, T., Tomoda, K., and Yamanaka, S. (2007) Induction of pluripotent stem cells from adult human fibroblasts by defined factors. *Cell* **131**, 861–872
3. Fazel, S., Cimini, M., Chen, L., Li, S., Angoulvant, D., Fedak, P., Verma, S., Weisel, R.D., Keating, A., and Li, R.K. (2006) Cardioprotective c-kit+ cells are from the bone marrow and regulate the myocardial balance of angiogenic cytokines. *J. Clin. Invest.* **116**, 1885–1877
4. Rosenzweig, A. (2006) Cardiac cell therapy-mixed results from mixed cells. *N. Engl. J. Med.* **355**, 1274–1277
5. Wollert, K.C., Meyer, G.P., Lotz, J., Lichtenberg, S.R., Lippolt, P., Breidenbach, C., Fichtner, S., Korte, T., Hornig, B., Messinger, D., Arseniev, L., Hertenstein, B., Ganser, A., and Drexler, H. (2004) Intracoronary autologous bone-marrow cell transfer after myocardial infarction: the BOOST randomised controlled clinical trial. *Lancet* **364**, 141–148
6. Schächinger, V., Erbs, S., Elsässer, A., Haberbosch, W., Hambrecht, R., Hölschermann, H., Yu, J., Corti, R., Mathey, D.G., Hamm, C.W., Suselbeck, T., Assmus, B., Tonn, T., Dimmeler, S., and Zeiher, A.M. (2006) Intracoronary bone marrow-derived progenitor cells in acute myocardial infarction. *N. Engl. J. Med.* **355**, 1210–1221
7. Assmus, B., Honold, J., Schächinger, V., Britten, M.B., Fischer-Rasokat, U., Lehmann, R., Teupe, C., Pistorius, K., Martin, H., Abolmaali, N.D., Tonn, T., Dimmeler, S., and Zeiher, A.M. (2006) Transcoronary transplantation of progenitor cells after myocardial infarction. *N. Engl. J. Med.* **355**, 1222–1232
8. Lunde, K., Solheim, S., Aakhus, S., Arnesen, H., Abdelnoor, M., Egeland, T., Endresen, K., Ilebekk, A., Mangschau, A., Fjeld, J.G., Smith, H.J., Taraldsrud, E., Grøgaard, H.K., Bjørnerheim, R., Brekke, M., Müller, C., Hopp, E., Ragnarsson, A., Brinchmann, J.E., and Forfang, K. (2006) Intracoronary injection of mononuclear bone marrow cells in acute myocardial infarction. *N. Engl. J. Med.* **355**, 1199–1209
9. Janssens, S., Dubois, C., Bogaert, J., Theunissen, K., Deroose, C., Desmet, W., Kalantzi, M., Herbots, L., Sinnaeve, P., Dens, J., Maertens, J., Rademakers, F., Dymarkowske, S., Gheysens, O., Cleemput, J.V., Bormans, G., Nuyts, J., Belmans, A., Mortelmans, L., Boogaerts, M., and Van de Werf, F. (2006) Autologous bone marrow-derived stem-cell transfer in patients with ST-segment elevation myocardial infarction: double-blind, randomised controlled trial. *Lancet* **367**, 113–121

10. Peggs, K.S., Verfuerth, S., Pizzey, A., Khan, N., Guiver, M., Moss, P.A., and Mackinnon, S. Adoptive cellular therapy for early cytomegalovirus infection after allogeneic stem-cell transplantation with virus-specific T-cell lines. *Lancet* **362**, 1375–1377
11. Dazzi, F., van Laar, J.M., Cope, A., and Tyndall, A. (2007) Cell therapy for autoimmune diseases. *Arthritis Res. Ther.* **9**, 206–214
12. Ringdén, Ó., Uzunel, M., Rasmusson, I., Remberger, M., Sundberg, B., Lönnies, H., Marschall, H.-U., Dlugosz, A., Szakos, A., Hassan, Z., Omazic, B., Aschan, J., Barkholt, L., and Le Blanc, K. (2006) Mesenchymal stem cells for treatment of therapy-resistant graft-versus-host disease. *Transplantation* **81**, 1390–1397
13. Derfoul, A., Perkins, G.L., Hall, D.J., and Tuan, R.S. (2006) Glucocorticoids promote chondrogenic differentiation of adult human mesenchymal stem cells by enhancing expression of cartilage extracellular matrix genes. *Stem Cells* **24**, 1487–1495
14. Nuttelman, C.R., Tripodi, M.C., and Anseth, K.S. (2004) *In vitro* osteogenic differentiation of human mesenchymal stem cells photoencapsulated in PEG hydrogels. *J. Biomed. Mater. Res. A* **68**, 773–782
15. Kulterer, B., Friedl, G., Jandrositz, A., Sanchez-Cabo, F., Prokesch, A., Paar, C., Scheideler, M., Windhager, R., Preisegger, K.-H., and Trajanoski, Z. (2007) Gene expression profiling of human mesenchymal stem cells derived from bone marrow during expansion and osteoblast differentiation. *BMC Genomics* **8**, 70–84
16. Pittenger, M.F., Mackay, A.M., Beck, S.C., Jaiswal, R.K., Douglas, R., Mosca, J.D., Moorman, M.A., Simonetti, D.W., Craig, S., and Marshak, D.R. (1999) Multilineage potential of adult human mesenchymal stem cells. *Science* **284**, 143–147
17. Barrett, T., Troup, D.B., Wilhite, S.E., Ledoux, P., Rudnev, D., Evangelista, C., Kim, I.F., Soboleva, A., Tomashevsky, M., and Edgar, R. (2007) NCBI GEO: mining tens of millions of expression profiles-database and tools update. *Nucleic Acids Res.* **35**, D760–D765
18. Edgar, R., Domrachev, M., and Lash, A.E. (2002) Gene Expression Omnibus: NCBI gene expression and hybridization array data repository. *Nucleic Acids Res.* **30**, 207–210
19. Toda, K., Ishida, S., Nakata, K., Matsuda, R., Shigemoto-Mogami, Y., Fujishita, K., Ozawa, S., Sawada, J., Inoue, K., Shudo, K., and Hayashi, Y. (2003) Test of significant differences with a priori probability in microarray experiments. *Anal. Sci.* **19**, 1529–1535
20. Benini, S., Perbal, B., Zambelli, D., Colombo, M.P., Manara, M.C., Serra, M., Parenza, M., Martinez, V., Picci, P., and Scotlandi, K. (2005) In Ewing's sarcoma CCN3(NOV) inhibits proliferation while promoting migration and invasion of the same cell type. *Oncogene* **24**, 4349–4361
21. Heymans, S., Lupu, F., Terclavers, S., Vanwetswinkel, B., Herbert, J.-M., Baker, A., Collen, D., Carmeliet, P., and Moons, L. (2005) Loss or inhibition of uPA or MMP-9 attenuates LV remodeling and dysfunction after acute pressure overload in mice. *Am. J. Pathol.* **166**, 15–25
22. Mundlos, S., Otto, F., Mundlos, C., Mulliken, J.B., Aylsworth, A.S., Albright, S., Lindhout, D., Cole, W.G., Henn, W., Knoll, J.H.M., Owen, M.J., Mertelsmann, R., Zabel, B.U., and Olsen, B.R. (1997) Mutaions involving the transcription factor CBFA1 cause cleidocranial dysplasia. *Cell* **89**, 773–779
23. Yamamura, Y., Lee, W.L., Inoue, K., Ida, H., and Ito, Y. (2006) RUNX3 cooperates with FoxO3a to induce apoptosis in gastric cancer cells. *J. Biol. Chem.* **281**, 5267–5276
24. Hu, B., Wang, S., Zhang, Y., Feghali, C.A., Dingman, J.R., and Wright, T.M. (2003) A nuclear target for interleukin-1α: Interaction with the growth suppressor necdin modulates proliferation and collagen expression. *Proc. Natl. Acad. Sci. USA* **100**, 10008–10013
25. Chen, C.-J., Kono, H., Golenbock, D., Reed, G., Akira, S., and Rock, K.L. (2007) Identification of a key pathway required for the sterile inflammatory response triggered by dying cells. *Nat. Med.* **13**, 851–856
26. Wan, D., Gong, Y., Qin, W., Zhang, P., Li, J., Wei, L., Zhou, X., Li, H., Qiu, X., Zhong, F., He, L., Yu, J., Yao, G., Jiang, H., Qian, L., Yu, Y., Shu, H., Chen, X., Xu, H., Guo, M., Pan, Z., Chen, Y., Ge, C., Yang, S., and Gu, J. (2004) Large-scale cDNA transfection screening for genes related to cancer development and progression. *Proc. Natl. Acad. Sci. USA* **101**, 15724–15729
27. Herath, N.I., Spanevello, M.D., Sabesan, S., Newton, T., Cummings, M., Duffy, S., Lincoln, D., Boyle, G., Parsons, P.G., and Boyd, A.W. (2006) Over-expression of Eph and ephrin genes in advanced ovarian cancer: ephrin gene expression correlates with shortened survival. *BMC Cancer* **6**, 144–150
28. Woelfle, U., Cloos, J., Sauter, G., Riethdorf, L., Jänicke, F., van Diest, P., Brakenhoff, R., and Pantel, K. (2003) Molecular signature associated with bone marrow micrometastasis in human breast cancer. *Cancer Res.* **63**, 5679–5684
29. Lin, C.G., Chen, C.-C., Leu, S.-J., Grzeszkiewicz, T.M., and Lau, L.F. (2005) Integrin-dependent functions of the angiogenic inducer NOV (CCN3). *J. Biol. Chem.* **280**, 8229–8237
30. Huang, Y., Haraguchi, M., Lawrence, D.A., Border, W.A., Yu, L., and Noble, N.A. (2003) A mutant, noninhibitory plasminogen activator inhibitor type 1 decreases matrix accumulation in experimental glomerulonephritis. *J. Clin. Invest.* **112**, 379–388
31. Sakamoto, K., Yamaguchi, S., Ando, R., Miyawaki, A., Kabasawa, Y., Takagi, M., Li, C.L., Perbal, B., and Katsube, K. (2002) The nephroblastoma overexpressed gene (NOV/ccn3) protein associates with Notch1 extracellular domain and inhibits myoblast differentiation via Notch signalling pathway. *J. Biol. Chem.* **277**, 29399–29405
32. Scherberich, A., Galli, R., Jaquiery, C., Farhadi, J., and Martin, I. (2007) 3D perfusion culture of human adipose tissue-derived endothelial and osteoblastic progenitors generates osteogenic constructs with intrinsic vascularization capacity. *Stem Cells* **25**, 1823–1829

J Epidemiol 2008; 18(3) 97-110
doi:10.2188/jea.JE2007432

Original Article

Effects of Airborne Particulate Matter on Respiratory Morbidity in Asthmatic Children

Lu Ma,[1] Masayuki Shima,[1] Yoshiko Yoda,[1] Hirono Yamamoto,[2] Satoshi Nakai,[2] Kenji Tamura,[3] Hiroshi Nitta,[3] Hiroko Watanabe,[4] and Toshiyuki Nishimuta.[4]

[1] Department of Public Health, Hyogo College of Medicine.
[2] Graduate School of Environment and Information Sciences, Yokohama National University.
[3] Environmental Health Science Division, National Institute for Environmental Studies.
[4] Department of Pediatrics, Shimoshizu National Hospital.

Received October 29, 2007; accepted December 19, 2007; released online May 16, 2008

ABSTRACT

Background: The effects of airborne particulate matter (PM) are a major human health concern. In this panel study, we evaluated the acute effects of exposure to PM on peak expiratory flow (PEF) and wheezing in children.

Methods: Daily PEF and wheezing were examined in 19 asthmatic children who were hospitalized in a suburban city in Japan for approximately 5 months. The concentrations of PM less than 2.5 μm in diameter ($PM_{2.5}$) were monitored at a monitoring station proximal to the hospital. Moreover, $PM_{2.5}$ concentrations inside and outside the hospital were measured using the dust monitor with a laser diode ($PM_{2.5(LD)}$). The changes in PEF and wheezing associated with PM concentration were analyzed.

Results: The changes in PEF in the morning and evening were significantly associated with increases in the average concentration of indoor $PM_{2.5(LD)}$ 24 h prior to measurement (-2.86 L/min [95%CI: -4.12, -1.61] and -3.59 L/min [95%CI: -4.99, -2.20] respectively, for 10-$\mu g/m^3$ increases). The change in PEF was also significantly associated with outdoor $PM_{2.5(LD)}$ concentrations, but the changes were smaller than those observed for indoor $PM_{2.5(LD)}$. Changes in PEF and concentration of stationary-site $PM_{2.5}$ were not associated. The prevalence of wheezing in the morning and evening were also significantly associated with indoor $PM_{2.5(LD)}$ concentrations (odds ratios = 1.014 [95%CI: 1.006, 1.023] and 1.025 [95%CI: 1.013, 1.038] respectively, for 10-$\mu g/m^3$ increases). Wheezing in the evening was significantly associated with outdoor $PM_{2.5(LD)}$ concentration. The effects of indoor and outdoor $PM_{2.5(LD)}$ remained significant even after adjusting for ambient nitrogen dioxide concentrations.

Conclusion: Indoor and outdoor $PM_{2.5(LD)}$ concentrations were associated with PEF and wheezing among asthmatic children. Indoor $PM_{2.5(LD)}$ had a more marked effect than outdoor $PM_{2.5(LD)}$ or stationary-site $PM_{2.5}$.

Key words: Particulate Matter, Asthma, Peak Expiratory Flow Rate, Respiratory Sounds.

INTRODUCTION

The effects of airborne particulate matter (PM) on human health have become a major concern.[1-3] Numerous previous panel studies have evaluated the acute effects of short-term exposure to PM on exacerbation of asthma in children in Western countries.[4-14] These studies have reported a relationship between elevated concentrations of PM and an increase in respiratory symptoms[4-10] as well as decreased pulmonary function values.[5,8,9,11-14] Many of these studies have examined the effects of PM with aerodynamic diameter less than 10 μm (PM_{10}). Recently, it has been reported that fine particles may have more adverse effects on respiratory symptoms and pulmonary functions than coarse particles.[15,16] Air quality standards for atmospheric concentrations of PM less than 2.5 μm in diameter ($PM_{2.5}$) have been established in the United States and European countries.[17] In Japan, many epidemiologic researches have dealt with the chronic effects of long-term exposure to air pollutants.[18-20] However, only a few studies have investigated the acute effects of short-term exposure to PM.[21,22]

Address for correspondence: Masayuki Shima, Department of Public Health, Hyogo College of Medicine, 1-1 Mukogawa-cho, Nishinomiya, Hyogo 663-8501, Japan. (e-mail: shima-m@hyo-med.ac.jp)

With respect to exposure assessment, in most previous studies, subjects were usually assigned concentrations measured at central regional sites or other outdoor sites. Use of central regional PM concentrations may lead to exposure misclassification and diminish the accuracy of exposure-response estimates. Many people spend most of their time indoors, where they are exposed to a combination of indoor-generated PM and outdoor-originated PM that has infiltrated the house.[23,24] Indoor concentrations of PM often differ from outdoor PM concentrations.[24-26] Therefore, to improve the accuracy of the estimated associations, concentrations of PM in the environment in which the subjects spend the majority of their time should be evaluated.

In this panel study, we evaluated the potential relationship between exposure to PM and asthma exacerbation in children who were hospitalized in a suburban city in Japan. The concentrations of PM were monitored inside and outside the hospital and at a monitoring station proximal to the hospital. To assess the acute effects of PM, we evaluated peak expiratory flow (PEF) and wheezing in the children.

METHODS

Subjects

The subjects of this panel study were 19 children aged 8-15 years, who had physician-diagnosed severe asthma and were hospitalized at Shimoshizu National Hospital in Yotsukaido City, Chiba Prefecture, Japan. Because the children had poorly controlled asthma with frequent exacerbations, they were under long-term hospitalization for maintenance medication for asthma, and attended a school for sick children, which was adjacent to the hospital. In November 2003, 19 children were under long-term hospitalization, and informed written consent was obtained from all the subjects and their parents. All of them had atopic disposition and received asthma medication, including inhaled corticosteroids (ICS). No major roads or factories were present in the vicinity of the hospital. This study was approved by the Medical Ethics Committee of Shimoshizu National Hospital.

Health Outcomes

PEF of all the children was evaluated daily using an electronic spirometer (AS-300; Minato Medical Science Inc., Tokyo, Japan). The measurements were conducted immediately prior to medication at least twice a day, i.e., in the morning (6:00 AM) and evening (7:00 PM), under the guidance of trained nurses. The presence or absence of wheezing was assessed based on auscultation by the trained nurses, and recorded with the results of PEF. For this study, we collected the records from November 5, 2003 through March 24, 2004.

Particulate Matter Measurements

To measure PM concentrations inside and outside the hospital, we used a digital dust monitor (LD-3K; Sibata Scientific Technology Inc., Tokyo, Japan), which is a portable monitor based on the light scattering principle, with a laser diode as the light source. The monitor determines the relative concentrations of PM by measuring the intensity of the laser beam scattered by particles. To convert the relative concentrations to mass concentrations of PM, conversion coefficients must be calculated based on the mass concentrations measured simultaneously using the filtration sampling method. We measured the mass concentrations of PM 7 times over a period of 24 h by using collocated portable air samplers (MP-Σ300; Sibata Scientific Technology Inc., Tokyo, Japan) equipped with cascade impactors (ATPS-20H; Sibata Scientific Technology Inc., Tokyo, Japan) with a flow rate of 1.5 L/min; the cut-off points of aerodynamic diameter were 2.5 μm and 10 μm ($PM_{2.5}$ and $PM_{2.5-10}$ respectively). The measurements by LD-3K strongly correlated with the concentrations of $PM_{2.5}$, and the R^2 value between them was 0.99 in the ward of the hospital and 0.93 at the entrance of the hospital, when compared with the mass concentrations based on the filtration sampling method. However, the measurements by LD-3K were not highly associated with the concentrations of coarse particles ($PM_{2.5-10}$) ($R^2 = 0.62$ and 0.51 in the ward of the hospital and at the entrance, respectively). Therefore, the respective conversion coefficients were calculated for PM concentrations inside or outside the hospital based on the relationship of the measurements of LD-3K to the mass concentrations of $PM_{2.5}$. The values ($PM_{2.5(LD)}$) converted by the coefficients were considered to be the approximate $PM_{2.5}$ concentrations.

During the study period, PM concentrations were continuously monitored using LD-3K in 2 hospital rooms, a hall in the children's ward, and at the entrance of the hospital. The average concentration of PM at the 3 sites in the hospital (2 hospital rooms and the hall of the ward) was regarded as the indoor $PM_{2.5(LD)}$ concentration, while the concentration at the entrance was regarded as the outdoor $PM_{2.5(LD)}$ concentration.

In addition, the concentration of $PM_{2.5}$ was measured with a tapered-element oscillating microbalance (TEOM; Thermo Electron Inc., East Greenbush, NY, USA) at a monitoring station proximal to the hospital. The concentrations of nitrogen dioxide (NO_2), temperature, and relative humidity were also measured continuously at the station. The distance between the hospital and the station was approximately 500 m.

Data Analysis

We used descriptive statistics of PM and NO_2 concentrations, temperature, and relative humidity, evaluated by correlation matrices for them. We examined daily measurements of PEF and wheezing in the asthmatic children in relation to the concentrations of PM and NO_2.

For regression analyses of daily PEF, we used the Generalized Estimating Equation (GEE),[27] which is suitable for correlated data in individuals.[28] The standard error of the regression estimate is adjusted for the possible correlation among the responses from 1 subject. This method generates robust estimators regardless of the specifications of the covariance matrix, and as autocorrelation is included in the covariance, coefficients can be interpreted as usual. The analyses for the measurements in the morning and evening were performed separately using each model. The results are demonstrated as the mean changes in PEF for 10-$\mu g/m^3$ or 10-ppb increments of PM or NO_2, respectively, after adjustment for sex, age (months), height (in November 2003), temperature, relative humidity, and growth of the children. Because only the heights of the children at the beginning of this study were available, we applied an ordinal variable, i.e., 1-5, to each month during this study (November 2003 through March 2004) as a surrogate for their growth. The minimum and maximum temperatures during the day were included in the model for the analyses of PEF in the morning and evening, respectively.

Exposure variables included the average concentration of each pollutant during the 12- or 24-h period preceding measurement. We also evaluated the effect of the 1-h maximum concentration of each pollutant in the 12-h period preceding measurement. We first performed the analyses with a single-pollutant model. Second, we carried out the analyses using 2-pollutant models, including NO_2 and one of the PM concentrations. Thereafter, to assess the potential of the delayed effects of PM, we also examined the effects of PM concentration on certain days before the day of PEF measurement; the number of days preceding measurement was termed as the number of lag days. This was accomplished by regressing PEF on PM concentrations measured every 24 or 12 h, upto 3 lag days.

We also used the GEE for analyzing the effects of pollutants on wheezing. Effect estimates for wheezing were expressed as odds ratios (ORs) with 95% confidence intervals (CIs) for 10-$\mu g/m^3$ or 10-ppb increments of PM or NO_2, respectively, after adjustment for sex, age (months), temperature, and relative humidity. In addition, the concentrations of each PM were categorized into quartiles and included in the model as dummy variables. The ORs and 95% CIs were calculated relative to the lowest quartile of each PM. The other procedures used for the analyses of wheezing were similar to those used for the analyses of PEF.

All statistical analyses were performed using the SPSS® 15.0 software (SPSS Inc., Chicago, IL, USA).

RESULTS

Descriptive Statistics

Table 1 shows the characteristics of the subjects and summarizes the daily measurements of PEF and records of wheezing in this study. The study population comprised 19 children (8 boys and 11 girls). The mean (standard deviation) PEF was 288.9 (75.5) L/min in the morning and 306.5 (75.1) L/min in the evening. The prevalence of wheezing, as noted in the medical records of the children, was 35.7% in the morning and 35.0% in the evening. Daily prevalence of wheezing is shown in Figure 1. In February 2004, a somewhat higher prevalence of wheezing was observed.

Table 2 describes the concentrations of PM and NO_2. The mean concentration of indoor $PM_{2.5(LD)}$ was higher during the nighttime than during the daytime. In comparison, the mean concentrations of outdoor $PM_{2.5(LD)}$ and stationary-site $PM_{2.5}$ during the daytime were similar to those during the nighttime. Daily concentrations of indoor and outdoor $PM_{2.5(LD)}$ and stationary-site $PM_{2.5}$ are also shown in Figure 1. At the beginning of February 2004, the concentrations of indoor $PM_{2.5(LD)}$ were considerably high. The concentration

Table 1. Descriptive statistics for the study subjects on the basis of sex.

	Male (n = 8)	Female (n = 11)	Total (n = 19)
Mean age (SD)(years)	12.4 (2.2)	13.3 (2.5)	12.9 (2.4)
Mean height* (SD) (cm)	150.6 (19.3)	147.4 (11.9)	148.8 (15.1)
Number of PEF measurements			
Morning, mean (SD)	81.9 (22.9)	88.4 (8.4)	85.6 (16.0)
Evening, mean (SD)	82.8 (22.0)	90.6 (6.9)	87.1 (15.5)
PEF			
Morning PEF, mean (SD) (L/min)	322.6 (88.2)	264.4 (57.1)	288.9 (75.5)
Evening PEF, mean (SD) (L/min)	333.7 (96.9)	284.8 (46.6)	306.5 (75.1)
Prevalence of wheezing			
Percentage in the morning (%)	33.8	37.2	35.7
Percentage in the evening (%)	36.4	33.8	35.0

SD, Standard deviation; PEF, peak expiratory flow.
* : Height in November 2003.

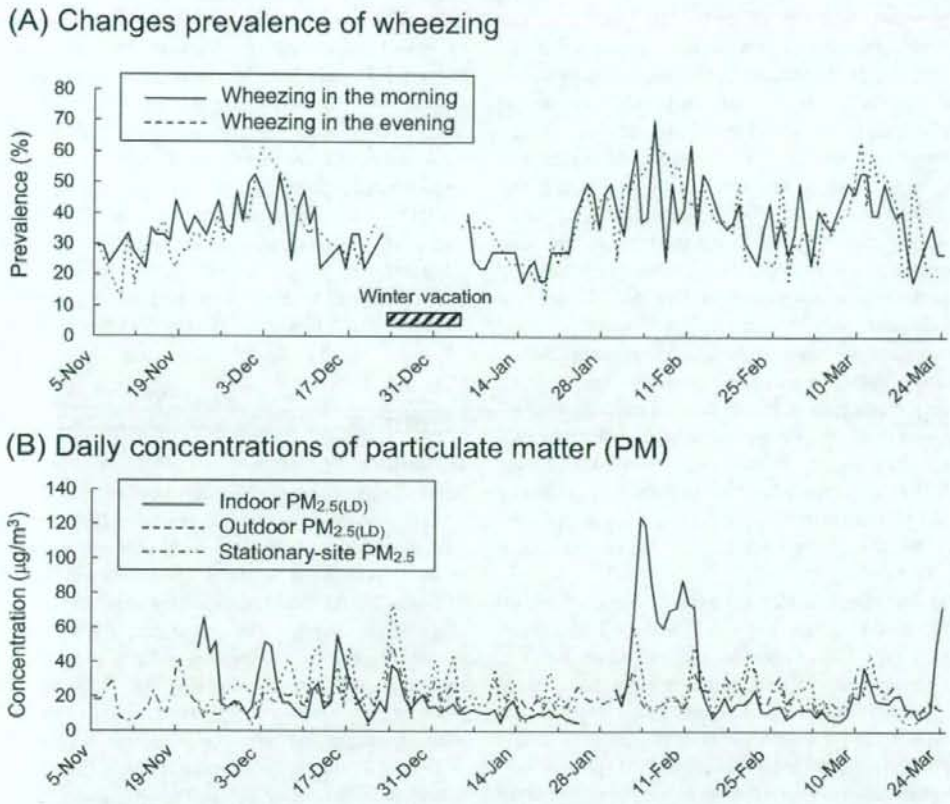

Figure 1. Daily prevalence of wheezing in the morning and evening (A) and daily concentrations of indoor and outdoor $PM_{2.5(LD)}$ and stationary-site $PM_{2.5}$ (24-h means) (B), from November 5, 2003 through March 24, 2004.

$PM_{2.5}$, particulate matter less than 2.5 μm in diameter; $PM_{2.5(LD)}$, $PM_{2.5}$ measured using the dust monitor with a laser diode.

of outdoor $PM_{2.5(LD)}$ was moderately correlated with the concentrations of stationary-site $PM_{2.5}$ and NO_2 (Table 3). However, the concentration of indoor $PM_{2.5(LD)}$ showed weak correlation with outdoor $PM_{2.5(LD)}$ concentration and no correlation with the concentrations of stationary-site $PM_{2.5}$ and NO_2.

Peak Expiratory Flow and Exposure to Particulate Matter

Table 4 shows the changes in PEF associated with a 10-$\mu g/m^3$ or 10-ppb increment in the concentration of each pollutant, using single-pollutant models adjusted for sex, age, height, temperature, relative humidity, and growth of the children. In 2-pollutant models including NO_2 concentration, in addition to the above factors, the changes in PEF in the morning and evening were also significantly associated with the increase in average concentrations of indoor $PM_{2.5(LD)}$ during the 24-h lag period. The changes in PEF were also significantly associated with the average concentration and 1-h maximum concentration of indoor $PM_{2.5(LD)}$ in the preceding 12 h. The change in PEF in the evening was larger than that in the morning. Moreover, some significant associations were present between the change in PEF and outdoor $PM_{2.5(LD)}$ concentrations, but the changes were smaller in relation to indoor $PM_{2.5(LD)}$ concentrations. The changes in PEF were not associated with stationary-site $PM_{2.5}$ or NO_2 concentrations. Two-pollutant models adjusted for NO_2 concentration showed similar associations between changes in PEF and PM concentrations.

Figure 2 shows the changes in PEF in relation to the average concentrations of PM for every 24 h, upto 3 lag days. The largest decreases in PEF in relation to the concentrations of indoor $PM_{2.5(LD)}$ were recorded for the morning and evening of the same day. The effects of indoor $PM_{2.5(LD)}$ on PEF were significant for upto 3 d in the morning and evening; however, the decreases in PEF became gradually smaller as

Table 2. Descriptive statistics of daily measurements of air pollutants and temperature during the study period.

Pollutants/temperature	n*	Mean	SD	Minimum	Median	Maximum
Indoor $PM_{2.5(LD)}$ ($\mu g/m^3$)						
24-h mean	119	24.6	23.2	5.3	15.3	124.5
12-h nighttime mean	119	28.3	33.8	4.5	15.2	181.1
12-h daytime mean	120	21.7	17.1	3.5	15.9	103.1
1-h nighttime maximum	119	44.7	52.1	5.5	23.8	238.9
1-h daytime maximum	120	41.5	42.2	4.6	24.3	192.9
Outdoor $PM_{2.5(LD)}$ ($\mu g/m^3$)						
24-h mean	118	22.6	12.7	3.3	20.3	73.5
12-h nighttime mean	118	21.7	16.3	1.7	16.7	92.1
12-h daytime mean	120	23.6	14.1	4.3	20.9	78.5
1-h nighttime maximum	118	34.0	23.6	2.9	29.0	136.4
1-h daytime maximum	120	38.6	22.6	5.6	35.0	110.9
Stationary-site $PM_{2.5}$ (TEOM)($\mu g/m^3$)						
24-h mean	136	19.1	7.8	3.5	18.1	49.9
12-h nighttime mean	141	17.2	8.5	2.6	16.7	56.4
12-h daytime mean	136	21.2	10.4	2.9	18.3	56.2
1-h nighttime maximum	141	28.5	14.8	4.9	25.6	95.8
1-h daytime maximum	136	35.8	15.8	4.9	33.7	110.8
Stationary-site NO_2 (ppb)						
24-h mean	141	20.6	7.7	6.5	21.1	41.0
12-h nighttime mean	141	21.8	9.7	3.3	21.1	42.6
12-h daytime mean	141	19.3	8.9	4.3	18.2	41.2
1-h nighttime maximum	141	31.6	11.9	5.0	32.0	57.0
1-h daytime maximum	141	31.5	11.9	5.0	32.0	56.0
Stationary-site temperature (℃)						
1-h maximum temperature	141	12.9	3.8	4.6	12.4	23.9
1-h minimum temperature	141	5.1	3.7	-0.8	4.2	15.2
Stationary-site relative humidity (%)						
24-h mean	141	61.4	15.9	28.0	60.0	93.0

SD, Standard deviation; $PM_{2.5}$, particulate matter less than 2.5 μm in diameter; $PM_{2.5(LD)}$, $PM_{2.5}$ measured using the dust monitor with a laser diode; TEOM, tapered-element oscillating microbalance; NO_2, nitrogen dioxide.
* : Some data are missing due to inefficient maintenance of the monitors or power failure.

Table 3. Correlation matrix of daily pollutants and temperature during the study period.

	Indoor $PM_{2.5(LD)}$, 24-h mean	Outdoor $PM_{2.5(LD)}$, 24-h mean	Stationary-site $PM_{2.5}$, 24-h mean	Stationary-site NO_2, 24-h mean	1-h maximum temperature	1-h minimum temperature	Relative humidity, 24-h mean
Indoor $PM_{2.5(LD)}$, 24-h mean	1	0.187 *	0.031	0.137	0.008	0.076	0.193 *
Outdoor $PM_{2.5(LD)}$, 24-h mean		1	0.674 **	0.585 **	0.155	0.132	0.393 **
Stationary-site $PM_{2.5}$, 24-h mean			1	0.473 **	0.173 *	-0.040	-0.051
Stationary-site NO_2, 24-h mean				1	-0.018	-0.123	0.053
1-h maximum temperature					1	0.775 **	0.300 **
1-h minimum temperature						1	0.527 **
Relative humidity, 24-h mean							1

The number of observations is 141 for stationary-site NO_2, temperature, and relative humidity; 136 for stationary-site $PM_{2.5}$; 119 for indoor $PM_{2.5(LD)}$; and 118 for outdoor $PM_{2.5(LD)}$.
$PM_{2.5}$, particulate matter less than 2.5 μm in diameter; $PM_{2.5(LD)}$, $PM_{2.5}$ measured using the dust monitor with a laser diode; NO_2, nitrogen dioxide.
* : $P<0.05$, ** : $P<0.01$

Table 4. Estimates and 95% confidence intervals (CIs) for change in peak expiratory flow (PEF) per 10-μg/m^3 or 10-ppb increase of each pollutant during the study period.

	Single-pollutant model*				Two-pollutant model †			
	Change ‡	95% CI		*P* value	Change ‡	95% CI		*P* value
				PEF in the morning				
Indoor $PM_{2.5(LD)}$								
24-h mean	-2.86	-4.12	-1.61	<0.001	-2.92	-4.23	-1.61	<0.001
12-h mean	-2.11	-3.02	-1.21	<0.001	-2.12	-3.04	-1.20	<0.001
1-h maximum in the preceding 12 h	-1.42	-2.03	-0.82	<0.001	-1.42	-2.03	-0.82	<0.001
Outdoor $PM_{2.5(LD)}$								
24-h mean	-1.34	-2.99	0.32	0.113	-1.96	-3.84	-0.09	0.040
12-h mean	-1.65	-3.18	-0.12	0.034	-2.04	-3.64	-0.44	0.013
1-h maximum in the preceding 12 h	-1.51	-2.59	-0.43	0.006	-1.88	-3.06	-0.69	0.002
Stationary-site $PM_{2.5}$								
24-h mean	-0.35	-1.89	1.20	0.662	0.01	-1.61	1.63	0.991
12-h mean	-0.54	-2.99	1.92	0.667	-0.55	-3.20	2.10	0.685
1-h maximum in the preceding 12 h	-1.03	-2.24	0.19	0.098	-1.34	-2.80	0.13	0.074
Stationary-site NO_2								
24-h mean	-0.68	-2.65	1.29	0.498	-			
12-h mean	-0.26	-1.96	1.44	0.761	-			
1-h maximum in the preceding 12 h	0.03	-1.21	1.26	0.968	-			
				PEF in the evening				
Indoor $PM_{2.5(LD)}$								
24-h mean	-3.59	-4.99	-2.20	<0.001	-3.59	-4.98	-2.20	<0.001
12-h mean	-4.92	-7.00	-2.85	<0.001	-4.96	-7.04	-2.89	<0.001
1-h maximum in the preceding 12 h	-2.22	-3.09	-1.36	<0.001	-2.23	-3.10	-1.37	<0.001
Outdoor $PM_{2.5(LD)}$								
24-h mean	-3.40	-6.47	-0.33	0.030	-4.00	-7.51	-0.49	0.025
12-h mean	-1.87	-3.85	0.11	0.064	-2.39	-4.75	-0.02	0.048
1-h maximum in the preceding 12 h	-0.65	-1.69	0.38	0.217	-0.48	-1.35	0.39	0.283
Stationary-site $PM_{2.5}$								
24-h mean	-1.38	-3.84	1.08	0.271	-0.28	-2.63	2.06	0.812
12-h mean	-0.72	-2.43	0.98	0.406	-0.80	-2.60	1.01	0.388
1-h maximum in the preceding 12 h	-0.73	-1.85	0.39	0.202	-0.45	-1.48	0.58	0.393
Stationary-site NO_2								
24-h mean	-1.69	-4.18	0.81	0.186	-			
12-h mean	-0.34	-2.66	1.98	0.774	-			
1-h maximum in the preceding 12 h	-1.27	-2.91	0.38	0.131	-			

$PM_{2.5}$, particulate matter less than 2.5 μm in diameter; $PM_{2.5(LD)}$, $PM_{2.5}$ measured using the dust monitor with a laser diode; NO_2, nitrogen dioxide.

* : The association between PEF and each pollutant was analyzed and adjusted for sex, age, height, temperature, relative humidity, and growth of the children.

† : The association between PEF and each pollutant was analyzed and adjusted for NO_2 concentration, sex, age, height, temperature, relative humidity, and growth of the children.

‡ : Mean changes in PEF (L/min) associated with a 10 μg/m^3 or 10 ppb increase of each pollutant.

the number of lag days increased. However, for a 1-d lag, the decrease in PEF in relation to the concentration of outdoor $PM_{2.5(LD)}$ was larger than that for the day of measurement. The associations were significant for 1- and 2-d lags in the morning and 0- and 1-d lags in the evening. No significant effects of stationary-site $PM_{2.5}$ on PEF were observed on the same day or upto 3 lag days either the morning or in the evening.

The changes in PEF in relation to the average concentrations of PM for every 12 h prior to measurement are also shown in Figure 2. Consistent decreases in PEF in the morning and evening were observed in relation to increases in indoor $PM_{2.5(LD)}$ concentrations, upto 72 h prior to measurement. PEF showed the greatest decrease in the morning in relation to the indoor $PM_{2.5(LD)}$ concentration during the 12-24-h lag period. However, PEF showed the greatest decrease in the evening in relation to the indoor $PM_{2.5(LD)}$ concentration during the preceding 0-12 h. Thus,

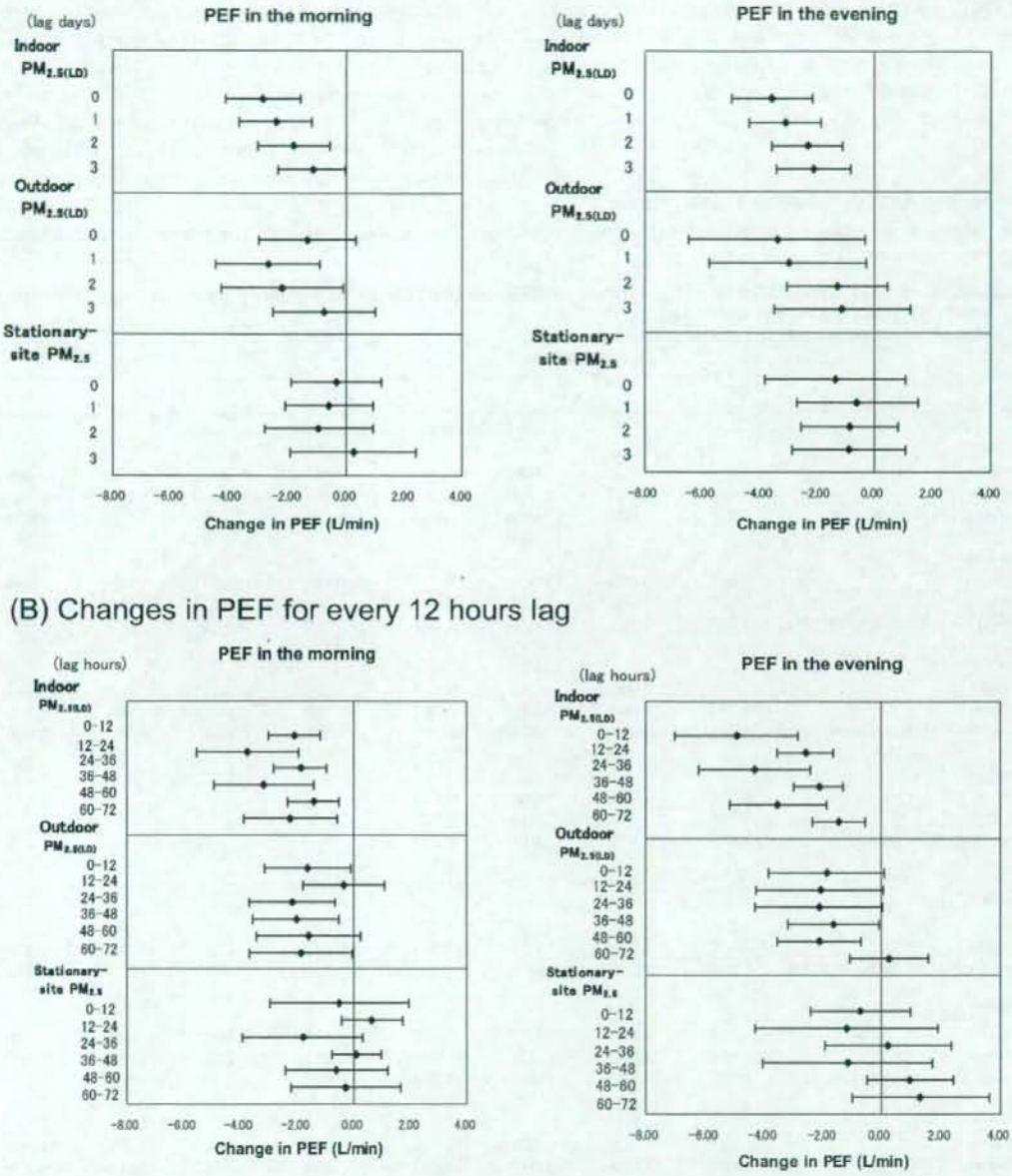

Figure 2. Changes in peak expiratory flow (PEF) in relation to the concentration of particulate matter (PM) for every 24 hours (A) and 12 hours (B), up to 3 days before the measurement (3 lag days).

Estimates for changes in PEF with 95% confidence intervals are shown per 10 $\mu g/m^3$ increase of each PM, adjusted for sex, age, height, temperature, relative humidity, and growth of the children.

the changes in PEF in relation to daytime indoor $PM_{2.5(LD)}$ concentrations were greater than those in relation to nighttime indoor $PM_{2.5(LD)}$ concentrations. With regard to the effect of outdoor $PM_{2.5(LD)}$ on PEF, the decreases in PEF in the morning and evening were greatest during the 24-36-h lag period. The changes in PEF were not related to the concentrations of stationary-site $PM_{2.5}$ during the 0-72-h lag period.

Wheezing and Exposure to Particulate Matter

Table 5 shows ORs for wheezing associated with a 10-$\mu g/m^3$ or 10-ppb increment of each pollutant. The prevalence of wheezing in the morning and evening was significantly associated with the average concentration of indoor $PM_{2.5(LD)}$ in the 24-h lag period. Wheezing was also significantly associated with both the average and 1-h maximum concentrations of indoor $PM_{2.5(LD)}$ in the preceding 12 h. The associations were stronger in the evening than in the morning. Wheezing in the evening was significantly associated with the average concentrations of outdoor $PM_{2.5(LD)}$ in the preceding 24 or 12 h. A few significant associations were also present between wheezing

Table 5. Adjusted odds ratios (ORs) and 95% confidence intervals (CIs) for wheezing per 10-$\mu g/m^3$ or 10-ppb increase in each pollutant during the study period.

	Single-pollutant model*				Two-pollutant model †			
	OR ‡	95% CI		*P* value	OR ‡	95% CI		*P* value
				Wheezing in the morning				
Indoor $PM_{2.5(LD)}$								
24-h mean	1.014	1.006	1.023	<0.001	1.015	1.006	1.024	<0.001
12-h mean	1.011	1.005	1.016	<0.001	1.011	1.005	1.017	<0.001
1-h maximum in the preceding 12 h	1.007	1.004	1.011	<0.001	1.007	1.004	1.011	<0.001
Outdoor $PM_{2.5(LD)}$								
24-h mean	0.993	0.980	1.006	0.271	0.997	0.983	1.010	0.624
12-h mean	1.001	0.988	1.014	0.888	1.002	0.990	1.015	0.707
1-h maximum in the preceding 12 h	1.003	0.994	1.011	0.559	1.003	0.993	1.012	0.591
Stationary-site $PM_{2.5}$								
24-h mean	1.014	0.987	1.042	0.301	1.020	0.978	1.063	0.363
12-h mean	1.013	1.000	1.026	0.052	1.020	0.995	1.046	0.119
1-h maximum in the preceding 12 h	1.014	0.997	1.031	0.119	1.015	0.993	1.038	0.184
Stationary-site NO_2								
24-h mean	0.995	0.971	1.019	0.670	-			
12-h mean	0.998	0.979	1.016	0.808	-			
1-h maximum in the preceding 12 h	1.002	0.991	1.014	0.675	-			
				Wheezing in the evening				
Indoor $PM_{2.5(LD)}$								
24-h mean	1.025	1.013	1.038	<0.001	1.025	1.012	1.038	<0.001
12-h mean	1.040	1.020	1.060	<0.001	1.040	1.020	1.062	<0.001
1-h maximum in the preceding 12 h	1.016	1.008	1.024	<0.001	1.016	1.008	1.025	<0.001
Outdoor $PM_{2.5(LD)}$								
24-h mean	1.016	1.002	1.029	0.024	1.010	0.996	1.026	0.170
12-h mean	1.014	1.002	1.026	0.022	1.017	1.001	1.033	0.041
1-h maximum in the preceding 12 h	1.002	0.992	1.011	0.739	0.998	0.988	1.009	0.764
Stationary-site $PM_{2.5}$								
24-h mean	1.033	1.008	1.058	0.009	1.027	0.984	1.073	0.219
12-h mean	1.022	1.004	1.042	0.019	1.024	0.994	1.055	0.116
1-h maximum in the preceding 12 h	1.006	0.997	1.016	0.177	1.002	0.990	1.014	0.700
Stationary-site NO_2								
24-h mean	1.024	0.996	1.052	0.093	-			
12-h mean	1.011	0.990	1.033	0.293	-			
1-h maximum in the preceding 12 h	1.014	1.001	1.028	0.035	-			

$PM_{2.5}$, particulate matter less than 2.5 μm in diameter; $PM_{2.5(LD)}$, $PM_{2.5}$ measured using the dust monitor with a laser diode; NO_2, nitrogen dioxide.

* : The association between wheezing and each pollutant was analyzed and adjusted for sex, age, temperature, and relative humidity.

† : The association between wheezing and each pollutant was analyzed and adjusted for NO_2 concentration, sex, age, temperature, and relative humidity.

‡ : ORs for wheezing associated with a 10 $\mu g/m^3$ or 10 ppb increase of each pollutant.

Table 6. Adjusted odds ratios (ORs) and 95% confidence intervals (CIs) for wheezing, in relation to quatiles of 24-h mean concentrations of each particulate matter (PM) during the study period.

	Wheezing in the morning			Wheezing in the evening		
	OR*	95% CI		OR*	95% CI	
Indoor $PM_{2.5(LD)}$, 24-h mean ($\mu g/m^3$)						
<11.0	1.000			1.000		
11.0-15.3	1.053	0.989	1.121	1.098	1.038	1.161
15.4-27.9	1.092	1.034	1.153	1.137	1.052	1.228
≥28.0	1.081	1.021	1.144	1.217	1.100	1.345
P value	0.011			0.002		
Outdoor $PM_{2.5(LD)}$, 24-h mean ($\mu g/m^3$)						
<13.0	1.000			1.000		
13.0-20.3	0.960	0.895	1.029	1.022	0.954	1.094
20.4-28.9	0.954	0.910	1.001	1.022	0.983	1.063
≥29.0	0.983	0.940	1.029	1.035	0.990	1.081
P value	0.208			0.474		
Stationary-site $PM_{2.5}$, 24-h mean ($\mu g/m^3$)						
<13.9	1.000			1.000		
13.9-18.1	1.029	0.960	1.103	1.010	0.957	1.067
18.2-23.5	1.015	0.957	1.077	1.062	1.017	1.109
≥23.6	1.015	0.947	1.088	1.094	1.032	1.160
P value	0.822			0.010		

$PM_{2.5}$, particulate matter less than 2.5 μm in diameter; $PM_{2.5(LD)}$, $PM_{2.5}$ measured using the dust monitor with a laser diode.
*: ORs for wheezing relative to the lowest quartile of each PM, adjusted for sex, age, temperature, and relative humidity.

in the evening and stationary-site $PM_{2.5}$. However, the associations between wheezing and stationary-site $PM_{2.5}$ were not significant in the 2-pollutant models adjusted for NO_2 concentration. Table 6 shows the ORs for wheezing relative to the lowest quartile of each PM in the preceding 24 h. Indoor $PM_{2.5(LD)}$ concentrations of 15.4 $\mu g/m^3$ or higher were significantly associated with increased wheezing in the morning. Wheezing in the evening was associated with indoor $PM_{2.5(LD)}$ concentrations ≥11.0 $\mu g/m^3$ and stationary-site $PM_{2.5}$ concentrations ≥18.2 $\mu g/m^3$.

Figure 3 shows the associations between wheezing and the average concentrations of PM for every 24 h upto 3 lag days. The prevalence of wheezing in the morning and evening significantly increased in relation to the increase in indoor $PM_{2.5(LD)}$ concentrations for 0-3 d lags. The association of ORs for wheezing in the morning with outdoor $PM_{2.5(LD)}$ gradually increased for 0-2 d lags, and the association with the 2-d lag was significant. The association between wheezing in the evening and outdoor $PM_{2.5(LD)}$ was significant only for the same day. Wheezing in the evening was also significantly related to the concentration of stationary-site $PM_{2.5}$ on the same day.

The association of wheezing with the average concentrations of PM for every 12 h preceding measurement is also shown in Figure 3. In the morning and evening, the associations between wheezing and indoor $PM_{2.5(LD)}$ concentrations were consistently significant for upto 72 h prior to measurement. The effects of indoor $PM_{2.5(LD)}$ concentration on wheezing were greater during the daytime than during nighttime. Some significant associations were present between wheezing and the concentrations of outdoor $PM_{2.5(LD)}$ and stationary-site $PM_{2.5}$, although these associations were not consistently observed.

DISCUSSION

In this panel study, we evaluated the acute effects of short-term exposure to PM by daily measurements of PEF and wheezing among asthmatic children in a hospital in a suburban city. All the children had been hospitalized for several months and attended a school for sick children, which was adjacent to the hospital. Because they spent almost the entire day in the hospital or school, their exposure levels to PM were considered to be nearly equal. Although all the children received asthma medication including ICS, they showed significant decreases in PEF and increases in wheezing after indoor or outdoor $PM_{2.5(LD)}$ concentrations were elevated. In particular, PEF and wheezing were shown to have consistent and strong associations with indoor $PM_{2.5(LD)}$ concentrations. The effects of indoor and outdoor $PM_{2.5(LD)}$ concentrations remained significant even after adjusting for ambient NO^2 concentrations.

Numerous studies have previously reported that PEF among asthmatics significantly decreases in relation to an increase in daily PM concentration.[5,8,9,11,13,15,29] With respect to the effects of fine particles, Romieu et al[9] evaluated the changes in daily PEF in relation to increases in $PM_{2.5}$ in a panel of

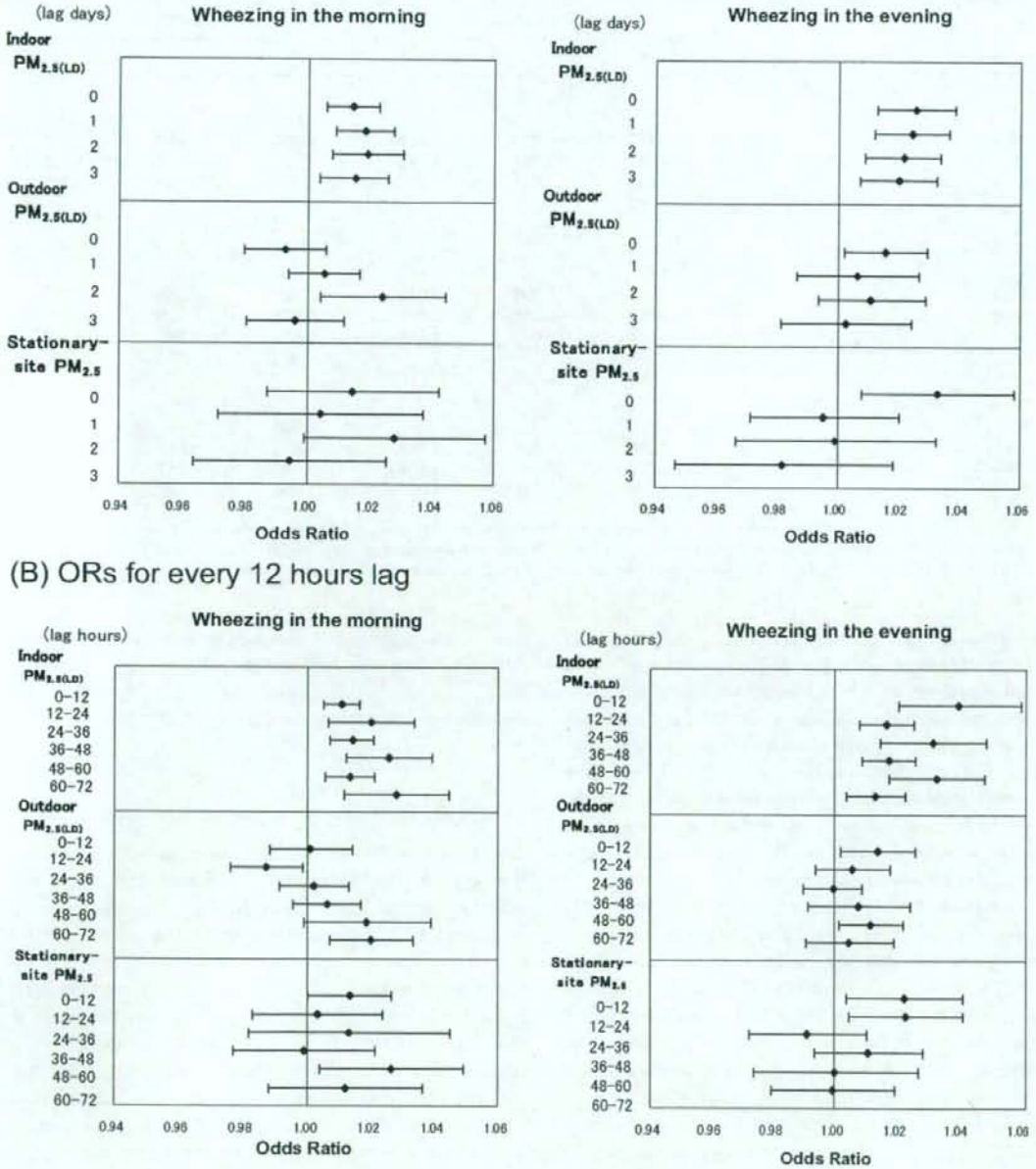

Figure 3. Odds ratios (ORs) for wheezing in relation to the concentration of particulate matter (PM) for every 24 hours (A) and 12 hours (B), up to 3 days before the measurement (3 lag days).

ORs with 95% confidence intervals are shown per 10 μg/m^3 increase of each PM, adjusted for sex, age, temperature, and relative humidity.